Research Article

High Reliability and Fast-Speed Phase-Change Memory Based on $Sb_{70}Se_{30}$/SiO_2 Multilayer Thin Films

Dan Zhang,[1] Yifeng Hu,[2] Haipeng You,[2] Xiaoqin Zhu,[2] Yuemei Sun,[2] Hua Zou,[2] and Yan Zheng [3]

[1]*School of Materials and Engineering, Jiangsu University of Technology, Changzhou 213001, China*
[2]*School of Mathematics and Physics, Jiangsu University of Technology, Changzhou 213001, China*
[3]*School of Automotive and Traffic Engineering, Jiangsu University of Technology, Changzhou, Jiangsu 213001, China*

Correspondence should be addressed to Yan Zheng; zy30003333@163.com

$Sb_{70}Se_{30}$/SiO_2 multilayer thin films were applied to improve the thermal stability by RF magnetron sputtering on SiO_2/Si (100) substrates. The characteristics of $Sb_{70}Se_{30}$/SiO_2 multilayer thin films were investigated in terms of crystallization temperature, ten years of data retention, and energy bandgap. It is observed that the crystallization temperature, 10-year data retention, and resistance of $Sb_{70}Se_{30}$/SiO_2 multilayer composite thin films exhibited a higher value, suggesting that $Sb_{70}Se_{30}$/SiO_2 multilayer composite thin films have superior thermal stability. The AFM measurement suggests that the SbSe (1 nm)/SiO (9 nm) multilayer thin films possess a smaller surface roughness (RMS = 0.23 nm). Besides, it was found that the phase-change time of SbSe (1 nm)/SiO (9 nm) multilayer thin films was shorter than that of GST in the process of crystallization and amorphization.

1. Introduction

With the increase of portable electronic devices, people's demand for volatile memory has increased dramatically [1]. Flash is now the mainstream of the nonvolatile memory market, but flash has several drawbacks such as its long operation time, the high voltage required for writing operations, and the fact used to store charges cannot meet the law of proportional reduction when it is very small [2–4]. Phase-change memory due to read and write with fast speed, high-density storage capacity, and compatible with complementary metal-oxide-semiconductor (CMOS), which regarded as the most promising alternative flash memory, becomes the mainstream of the next generation of nonvolatile storage technology [5, 6]. In order to solve the problems of large operation current and thermal interference, the whole development trend of PCM is in the three-dimensional direction to the nanometer scale. The sulfur compound semiconductor is a key portion of the phase-change memory currently, and its performance directly determines the performance of the phase-change memory [7, 8].

Until recently, $Ge_2Sb_2Te_5$ (GST) has been attracted much attention in PCM research due to its relatively good performance. However, $Ge_2Sb_2Te_5$ has some problems such as low crystallization temperature (~160°C) and poor data retention (~85°C for 10 years), which cannot meet the requirements of high-density storage in the future data age [9, 10]. To this end, various strategies such as doping and compositing have been performed to improve the performances of phase-change materials. In the case of nitrogen-doped GST, nitrogen is located in the grain vacancies or grain boundaries as a result of thermodynamic stability [11]. Nitrogen doping in $Sb_{70}Se_{30}$ film can raise its thermal stability, reducing the RESET current [12]. Additionally, Superlattice-like (SLL) Si/$Sb_{80}Te_{20}$ films have been confirmed to have a rapid crystallization speed [13]. Besides, previous studies [14–16] suggest that alternative multilayer phase-change materials can increase reversible phase-change speed and decrease the whole phase-change process power consumption, which is due to the fact condition that the advantages of different kinds of materials can be complementary.

In this study, $Sb_{70}Se_{30}/SiO_2$ (SbSe/SiO) multilayer thin films were fabricated by the radio frequency (RF) sputtering method. The thermal stability, crystallization characteristics, and optical transition of SbSe/SiO phase-change material were investigated in detail. The investigations of resistance versus temperature (R-T), X-ray diffraction (XRD), and surface topography measurements were carried out.

2. Experimental Details

In this work, SbSe/SiO multilayer thin films with different thickness ratios and $Sb_{70}Se_{30}$ and SiO_2 targets were deposited on SiO_2/Si (100) with a thickness of 0.5 cm substrates by the radio frequency (RF) magnetron sputtering system at room temperature. The purity of $Sb_{70}Se_{30}$ and SiO_2 targets was 99.9999%. Prior to the growth of thin films, the deposition rates of SbSe and SiO single layers were predetermined. The total thickness of SbSe/SiO thin films was 50 nm, and the periodicity was 5. The thickness of each individual layer can be designed by controlling the deposition time. The SbSe and SiO layers were deposited alternately to obtain the required number of layers of SbSe/SiO. The base pressure in the deposition chamber was 2×10^{-4} Pa. All deposition processes were carried out in Ar gas pressure of 0.4 Pa, the flow of 30 SCCM, and the RF power of 30 W. The substrate holder was rotated at an autorotation speed of 20 rpm to ensure the uniformity of deposition.

The amorphous-to-crystalline transition was investigated by in situ temperature-dependent resistance (R-T) measurement using a TP 95 temperature controller (Linkam Scientific Instruments Ltd., Surrey, UK) at a heating rate of 10°C/min. The size of each measured thin film is 1 cm × 1 cm. The electrode made up of Si_3N_4 is set up on the surface of the sample with a diameter of 0.7 μm, and the separation gap between two electrodes is 5 mm. The activation energy (E_a) and data retention temperature of ten years can be further gained by measuring the isothermal crystallization curve. The bandgap was obtained by measuring the reflectivity of thin films in the range of 400–2500 nm by the NIR spectrophotometer (7100CRT, XINMAO, China). The crystalline structures of the films were analyzed by X-ray diffraction (XRD, PANalytical, X'PERT Powder). The incidence angle θ ranges from 10° to 30°, and the diffraction patterns were taken in the 2θ range from 20° to 60° using Cu Kα radiation with a scanning step of 0.01°C/min. The surface morphology of the films was examined by atomic force microcopy (AFM, FMNanoview 1000). A picosecond laser pump-probe system was used to investigate the phase-change time between amorphous and crystalline states, by measuring the reflectivity of the material. The light source used for irradiating the samples was a frequency-doubled model-locked neodymium yttrium aluminum garnet laser operating at 532 nm wavelength at a pulse duration of 30 ps.

3. Results and Discussion

The resistance as a function of temperature (R-T) for SbSe/SiO multilayer thin films with different thickness ratios at a heating rate of 10°C/min is shown in Figure 1. As can be seen, all thin
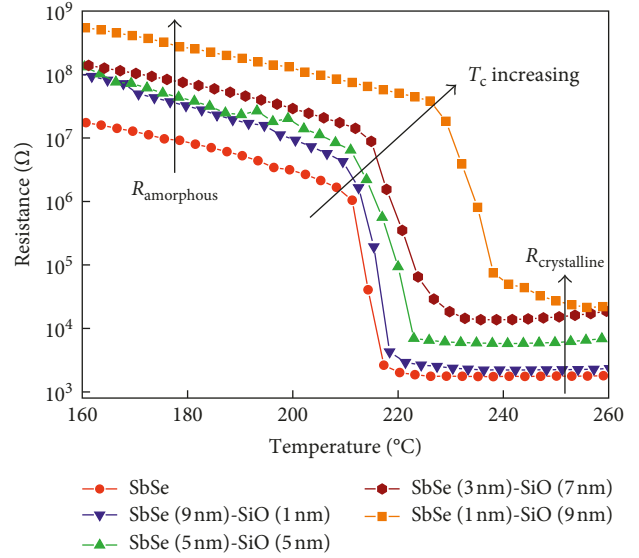

FIGURE 1: R-T curves of SbSe and SbSe/SiO multilayer thin films at a heating rate of 10°C/min.

films first display high resistance values, which are considered to be associated with semiconductor behavior. The resistance decreases sharply as the temperature reaches to a certain value which is referred to as the crystallization temperature T_c [17]. Figure 1 illustrates that with the increasing thickness of the SiO ratio, the T_c values of the SbSe/SiO thin films increase from 210°C to 228°C. This suggests that SiO deposition inhibits the crystallization and increases the crystallization temperature. As is known, the higher T_c represents better thermal stability [18]. Therefore, we can infer that SbSe/SiO multilayer thin films improve the thermal stability. Good thermal stability of the phase-change materials is beneficial to the data retention and the reliability of the PCM devices, which is of great significance in practical application. Besides, the resistances of amorphous and crystallization states were observed to increase with the thickness of the SiO_2 layer, which is helpful for reducing RESET current according to the joule heating equation [19]. Therefore, PCM devices based on SbSe/SiO multilayer thin films will have lower power consumption.

The plot of logarithm failure time versus $1/k_B T$, as shown in Figure 2, fits a linear Arrhenius relationship due to its thermal activation nature. In our case, the fitted straight line could be described as the following equation [20]:

$$t = \tau_0 \exp\left(\frac{E_a}{k_B T}\right), \tag{1}$$

where t, τ_0, k_B, and T are the failure time, a preexponential factor depending on the thin film's properties, the Boltzmann constant, and the absolute temperature, respectively. The extrapolated fitting lines show that the temperature for 10-year data retention of SbSe, SbSe (5 nm)/SiO (5 nm), SbSe (3 nm)/SiO (7 nm), and SbSe (1 nm)/SiO (9 nm) were 141°C, 160°C, 165°C, and 182°C, respectively. Comparing with SbSe thin films, SbSe/SiO multilayer thin films display better reliability of resistance state at higher temperature, which can meet the demands of data-storage applications at higher
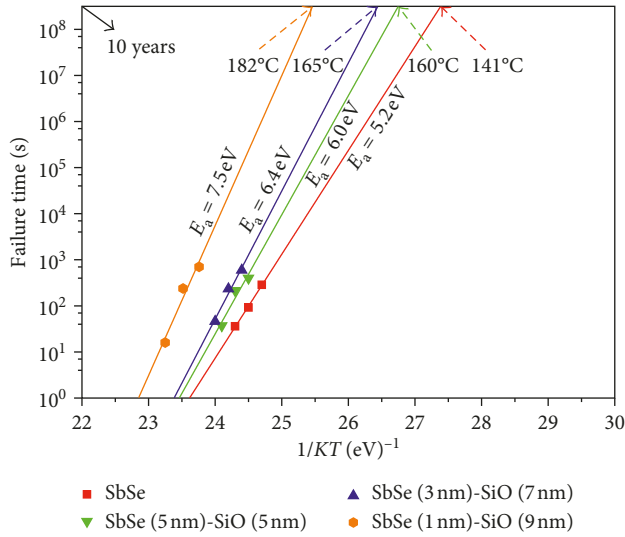
FIGURE 2: Plots of failure times as a function of reciprocal temperature of SbSe and SbSe/SiO multilayer thin films.

FIGURE 3: The Kubelka–Munk function of amorphous SbSe and SbSe (1 nm) SiO (9 nm) multilayer thin films.

temperature. The activation energy E_a for crystallization provides a good estimation of the archival life stability of an amorphous phase-change material. E_a for SbSe, SbSe (5 nm)/SiO (5 nm), SbSe (3 nm)/SiO (7 nm), and SbSe (1 nm)/SiO (9 nm) multilayer thin films, evaluated by the slope of the fitted curves presented in Figure 2, were 5.2, 6.0, 6.4, and 7.5 eV, respectively. Higher E_a implies better reliability of the amorphous phase. As shown in Figure 2, the 10-year data retention and E_a of SbSe/SiO multilayer films increase with the SiO thickness ratio, which indicate that SbSe/SiO multilayer film has the best reliability and is more qualified for PCM application.

The diffuse reflectivity spectra of SbSe thin film and SbSe/SiO multilayer thin films were measured by NIR spectrophotometry in the wavelength ranging from 400 to 2500 nm at room temperature [21]. The bandgap energy (E_g) could be determined by extrapolating the absorption edge onto the energy axis, as shown in Figure 3. The conversion of the reflectivity to absorbance data is obtained by the Kubelka–Munk function (K-M) [22]:

$$\frac{K}{S} = \frac{(1-R)^2}{2R}, \tag{2}$$

where R is the reflectivity, K is the absorption coefficient, and S is the scattering coefficient. As shown in Figure 3, the bandgap energy for SbSe, SbSe (5 nm)/SiO (5 nm), SbSe (3 nm)/SiO (7 nm), and SbSe (1 nm)/SiO (9 nm) multilayer thin films are 1.47, 1.53, 1.58, and 1.66 eV, respectively. With the increase of SiO thickness, E_g of amorphous films spreads more widely. In general, the carrier density inside the semiconductors is proportional to $\exp(-E_a/2KT)$ [23], and the increase of the bandgap will result in the reduction of carriers, which makes a major contribution to the increase of film resistivity. Thus, the activation energy for crystallization is increased, improving the stability of the amorphous phase. This finding is in accordance with the results from Figure 1.

The crystalline structure of SbSe and SbSe (1 nm) SiO (9 nm) thin films was characterized by XRD. Figure 4 shows
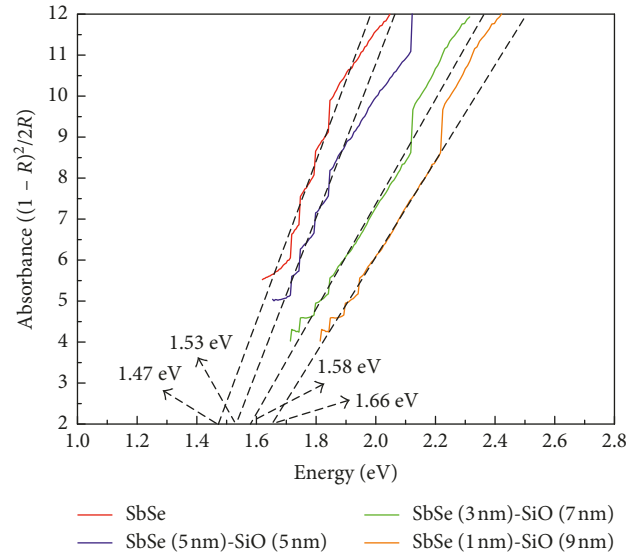
the XRD patterns of SbSe and SbSe (1 nm) SiO (9 nm) thin films annealed for 10 minutes at different temperatures. The different annealing temperatures correspond to different crystallization stages. As can be seen, there is no diffraction peak in all the as-deposited thin films, implying that the films have not crystallized at all and are still in the amorphous structure [24, 25]. After annealing above crystallization temperature T_c, multiple diffraction peaks are observed. The diffraction peak (211) belonging to Si appeared in SbSe and SbSe (1 nm) SiO (9 nm) thin films, which is associated with the SiO_2/Si substrate. As presented in Figure 4, the diffraction peak (012) belonging to Sb appears in SbSe and SbSe/SiO thin films, which suggests that Sb is excessive [4, 26]. From the XRD patterns of SbSe (1 nm) SiO (9 nm) multilayer thin films, it can be inferred that the SiO exists as the amorphous phase in all SbSe (1 nm) SiO (9 nm) multilayer thin films since no SiO diffraction peaks are observed [27], implying that the phase transition does not occur in the SiO layers. Due to the interface holding effect in the SbSe/SiO multilayer thin films, the SiO layers will impede the propagation of carriers and increase the resistance. This may suggest that SiO layers play an important role to improve the crystallization temperature and thermal stability. In general, the SbSe/SiO multilayer thin films have better thermal stability than SbSe thin film, which will be beneficial to the reliability of the PCRAM.

Film surface roughness is of great significance for the device performance due to the electrode–film interface affected by the induced stress during the phase-change process [28, 29]. The microstructures of the SbSe thin film and SbSe (1 nm)/SiO (9 nm) multilayer thin films before and after crystallization have been detected by AFM. The SbSe thin film and SbSe (1 nm)/SiO (9 nm) multilayer thin films were annealed at 240°C for 10 min. Figure 5 shows the AFM images of as-deposited and annealed SbSe thin film and SbSe (1 nm)/SiO (9 nm) multilayer thin films. The surfaces of amorphous SbSe thin film and SbSe (1 nm)/SiO (9 nm)
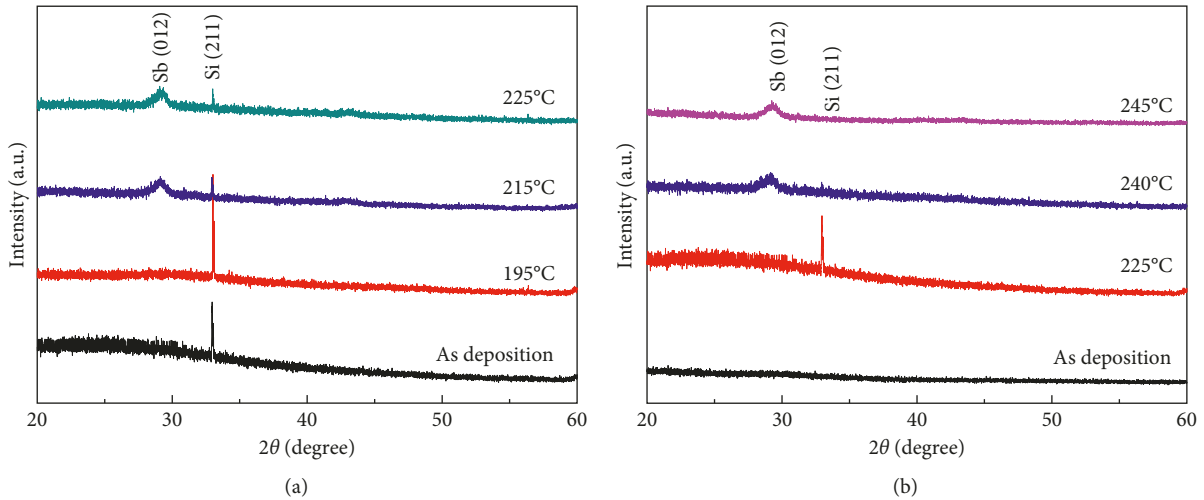
Figure 4: XRD patterns of thin films annealed at different temperatures for 10 min in Ar atmosphere: (a) SbSe and (b) SbSe (1 nm)/SiO (9 nm).
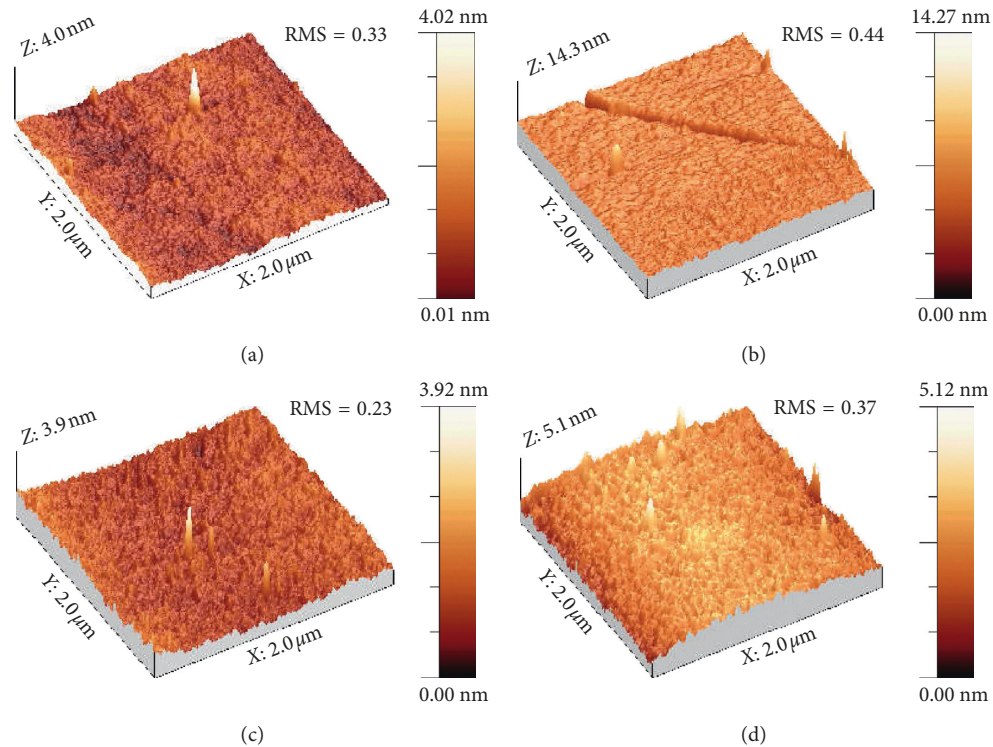

Figure 5: AFM topographic images: (a) SbSe; (b) annealed SbSe; (c) SbSe (1 nm)/SiO (9 nm); (d) annealed SbSe (1 nm)/SiO (9 nm).

multilayer thin films are smooth relatively, with the root-mean-square (RMS) surface roughness of 0.33 and 0.23 nm, respectively. After crystallization, the RMS of SbSe thin film increases to 0.44 nm. By contrast, the annealed SbSe (1 nm)/SiO (9 nm) multilayer thin film has a smaller RMS (0.37 nm). Above points imply that the internal stress change of SbSe (1 nm)/SiO (9 nm) multilayer thin film is much smaller, which is helpful to the fatigue performance of phase-change memory. These values of the RMS are lower than the other phase-change films, such as Sb_2–Te_3 [30] and $Ge_{10}Sb_{90}$ [31], indicating well smooth surface for PCM devices.

In the phase change, the electrical resistivity changes are accompanied by optical reflectivity. In this study, the switching speed of the phase-change materials was investigated by picosecond laser technology. Since the reset operation needs more power and shorter time than the set one in the resistance switching process of PCM devices, the reset power and the set speed have been attracted more attention [32]. That is to say, the power consumption and operation speed of PCM are mainly determined by the reset and set processes, respectively. Figure 6 shows the normalized reflectivity evolution of the SbSe (1 nm)/SiO (9 nm)
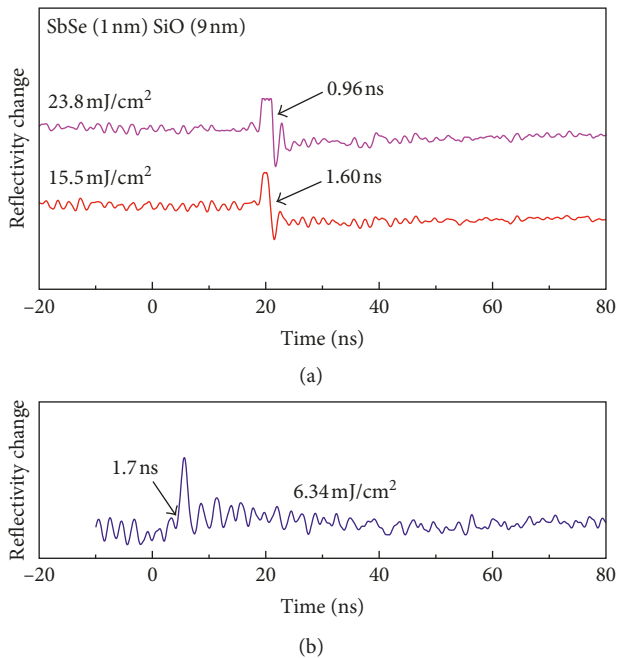
FIGURE 6: Reversible reflectivity evolution of SbSe (1 nm) SiO (9 nm) thin film: (a) amorphization and (b) crystallization.

multilayer thin film. In the picosecond laser test, the time of 0 is a reference for data recording, and it does not correspond to the time of phase transition. What is concerned in present study is the time interval from crystalline state to amorphous state which appears as abrupt change in reflectivity. As can be seen from Figure 6(a), the reflectivity dropped, implying the transition from crystalline-to-amorphous state. The amorphization time was 1.60 ns and 0.96 ns, which corresponds to the irradiation fluences of 15.5 mJ/cm^2 and 23.8 mJ/cm^2, respectively. As shown in Figure 6(b), the crystallization time was observed at 1.7 ns under the irradiation fluence of 6.34 mJ/cm^2. It has been reported that the crystallization time of GST is 23.1 ns [33]. Therefore, we can infer that the SbSe (1 nm)/SiO (9 nm) multilayer thin film possesses the faster phase-change speed.

4. Conclusion

In summary, SbSe/SiO multilayer thin films were prepared by the radio frequency (RF) sputtering method. Phase-change behavior was studied by in situ temperature-dependent resistance measurements. The crystallization temperature, activation energy, and 10-year data retention temperature of the SbSe/SiO multilayer thin films were proved to be larger than those of conventional SbSe thin film, which indicates the SbSe/SiO multilayer thin films have better thermal stability in comparison with SbSe thin film. The AFM measurement shows that the SbSe (1 nm)/SiO (9 nm) multilayer thin films possess better surface roughness (0.23 nm) than that of SbSe thin film. Meanwhile, the picosecond laser measurement suggests that the crystallization time of SbSe (1 nm)/SiO (9 nm) multilayer thin films is shorter than that of GST thin film. The results indicate that the SbSe/SiO multilayer thin films are a promising candidate for high-reliability and low-consumption PCM device applications.

Data Availability

The authors would like to share their original data in a native format (.xls and .txt). The data used to support the findings of this study can be directly obtained by requesting it from the corresponding author.

Conflicts of Interest

The authors declare that they have no conflicts of interest.

References

[1] H. Volker, P. Jost, and M. Wuttig, "Low-temperature transport in crystalline Ge$_1$Sb$_2$Te$_4$," *Advanced Functional Materials*, vol. 25, no. 40, pp. 6390–6398, 2015.

[2] Y. F. Hu, X. Q. Zhu, H. Zou et al., "Improved thermal stability of N-doped Sb materials for high-speed phase change memory application," *Applied Physics Letters*, vol. 108, no. 22, article 223103, 2016.

[3] Z. M. Sun, J. Zhou, and R. Ahuja, "Structure of phase change materials for data storage," *Physical Review Letters*, vol. 96, no. 5, article 055507, 2006.

[4] Y. G. Lu, S. N. Song, X. Shen, Z. T. Song, G. X. Wang, and S. X. Dai, "Study on phase change properties of binary GaSb doped Sb–Se film," *Thin Solid Films*, vol. 589, pp. 215–220, 2015.

[5] X. Q. Zhu, Y. F. Hu, H. Zou et al., "Si/Sb superlattice-like thin films for ultrafast and low power phase change memory application," *Scripta Materialia*, vol. 66, p. 121, 2016.

[6] Y. H. Zheng, Y. Cheng, M. Zhu et al., "A candidate Zr-doped Sb$_2$Te alloy for phase change memory application," *Applied Physics Letters*, vol. 108, no. 5, article 052107, 2016.

[7] G. X. Wang, Y. W Zhang, P. Liu, J. Wang, Q. H Nie, and X. Shen, "Phase change behavior of pseudo-binary ZnTe-ZnSb material," *Materials Letters*, vol. 213, pp. 342–345, 2018.

[8] K. Ren, R. H. Li, X. Chen et al., "Controllable SET process in O-Ti-Sb-Te based phase change memory for synaptic application," *Applied Physics Letters*, vol. 112, no. 7, article 073106, 2018.

[9] Z. F. He, W. H. Wu, X. Y. Liu et al., "Improvement of phase change properties of stacked Ge$_2$Sb$_2$Te$_5$/ZnSb thin films for phase change memory application," *Materials Letters*, vol. 185, pp. 399–402, 2016.

[10] Y. Q. Zhu, Z. H. Zhang, S. N. Song et al., "Ni-doped GST materials for high speed phase change memory applications," *Materials Research Bulletin*, vol. 64, 2015.

[11] Y. Lai, B. Qiao, J. Feng et al., "Nitrogen-doped Ge$_2$Sb$_2$Te$_5$ films for nonvolatile memory," *Journal of Electronic Materials*, vol. 34, no. 2, pp. 176–181, 2005.

[12] J. H. Park, J. H. Jeong, and D. J. Choi, "Study on the crystallization behavior of nitrogen-doped SbSe films for PCRAM applications," *Physica Status Solidi (A)*, vol. 213, no. 6, pp. 1526–1534, 2016.

[13] C. Z. Wang, J. W. Zhai, Z. T. Song, F. Shang, and X. Yao, "Phase-change behavior in $Si/Sb_{80}Te_{20}$ nanocomposite multilayer films," *Applied Physics A*, vol. 103, no. 1, pp. 193–198, 2011.

[14] Y. F. Hu, X. Y. Feng, S. M. Li et al., "Superlattice-like $Sb_{50}Se_{50}/Ga_{30}Sb_{70}$ thin films for high-speed and high density phase change memory application," *Applied Physics Letters*, vol. 103, no. 15, article 152107, 2013.

[15] M. Zhu, M. J. Xia, F. Rao et al., "One order of magnitude faster phase change at reduced power in Ti-Sb-Te," *Nature Communications*, vol. 5, no. 1, p. 4086, 2014.

[16] H. Tong, X. S. Miao, X. M. Cheng et al., "Thermal conductivity of chalcogenide material with superlatticelike structure," *Applied Physics Letters*, vol. 98, no. 10, article 101904, 2011.

[17] C. Wang, J. Zhai, Z. Song, F. Shang, and X. Yao, "Ge/Sb_2Te_3 nanocomposite multilayer films for high data retention phase-change random access memory application," *Applied Surface Science*, vol. 257, no. 3, pp. 949–953, 2010.

[18] Y. F. Hu, M. C. Sun, S. N. Song, Z. T. Song, and J. W. Zhai, "Oxygen-doped Sb_4Te phase change films for high-temperature data retention and low-power application," *Journal of Alloys and Compounds*, vol. 551, pp. 551–555, 2013.

[19] Y. G. Lu, S. N. Song, Z. T. Song, and B. Liu, "$Ga_{14}Sb_{86}$ film for ultralong data retention phase-change memory," *Journal of Applied Physics*, vol. 109, no. 6, article 064503, 2011.

[20] Y. F. Hu, Z. F. He, J. W. Zhai et al., "Superlattice-like $SnSb_4/Ga_3Sb_7$ thin films for ultrafast switching phase-change memory application," *Applied Physics A*, vol. 121, no. 3, pp. 1125–1131, 2015.

[21] C. C. Huang, B. Gholipour, K. Knight, J. Y. Ou, and D. W. Hewak, "Deposition and characterization of CVD-grown Ge-Sb thin film device for phase-change memory application," *Advances in OptoElectronics*, vol. 2012, Article ID 840348, 7 pages, 2012.

[22] Y. G. Lu, S. N. Song, Z. T. Song et al., "Superlattice-like $GaSb/Sb_2Te_3$ films for low-power phase change memory," *Scripta Materialia*, vol. 66, no. 9, pp. 702–705, 2012.

[23] X. Q. Zhu, Y. F. Hu, H. Zou et al., "Si/Sb superlattice-like thin films for ultrafast and low power phase change memory application," *Scripta Materialia*, vol. 121, pp. 66–69, 2016.

[24] C. Peng, Z. T. Song, F. Rao et al., "$Al_{1.3}Sb_3Te$ material for phase change memory application," *Applied Physics Letters*, vol. 99, no. 4, article 043105, 2011.

[25] S. Sharda, N. Sharma, P. Sharma, and V. Sharma, "Band gap and dispersive behavior of Ge alloyed a-SbSe thin films using single transmission spectrum," *Materials Chemistry and Physics*, vol. 134, no. 1, pp. 158–162, 2012.

[26] Y. G. Lu, S. N. Song, X. Shen et al., "Phase change characteristics of Sb-rich Ga–Sb–Se materials," *Journal of Alloys and Compounds*, vol. 586, pp. 669–673, 2014.

[27] Y. F. Gu, Y. Cheng, S. N. Song et al., "Advantages of Si_xSb_2Te phase-change material and its applications in phase-change random access memory," *Scripta Materialia*, vol. 65, no. 7, pp. 622–625, 2011.

[28] F. Wei, L. Wang, T. Kong et al., "Amorphous thermal stability of Al-doped Sb_2Te_3 films for phase-change memory application," *Applied Physics Letters*, vol. 103, no. 18, article 181908, 2013.

[29] W. H. Wu, Y. F. Hu, X. Q. Zhu et al., "High speed and low power consumption of superlattice-like $Ge/Sb_{70}Se_{30}$ thin films for phase change memory application," *Journal of Materials Science: Materials in Electronics*, vol. 27, no. 3, pp. 2183–2188, 2016.

[30] X. Cheng, L. Bo, S. Zhi-Tang, F. Song-Lin, and C. Bomy, "Characteristics of Sn-doped $Ge_2Sb_2Te_5$ films used for phase-change memory," *Chinese Physics Letters*, vol. 22, no. 11, pp. 2929–2932, 2005.

[31] H. Zou, Y. Hu, X. Zhu et al., "Improvement in reliability and power consumption based on $Ge_{10}Sb_{90}$ films through erbium doping," *Journal of Materials Science*, vol. 52, no. 9, pp. 5216–5222, 2017.

[32] Z. Y. Li, Y. F. Hu, T. Wen, J. W. Zhai, and T. S. Lai, "Femtosecond laser-induced crystallization of amorphous N-doped Ge_8Sb_{92} films and in situ characterization by coherent phonon spectroscopy," *Journal of Applied Physics*, vol. 117, no. 13, article 135703, 2015.

[33] W. H. Wu, Y. F. Hu, X. Q. Zhu et al., "Improvement of the thermal stability and power consumption of $Sb_{70}Se_{30}$ through nitrogen doping," *Journal of Materials Science: Materials in Electronics*, vol. 26, no. 12, pp. 9700–9706, 2015.

The Scientific World Journal

Journal of Applied Chemistry

Journal of Nanomaterials

Scientifica

International Journal of Polymer Science

Advances in Chemistry

Advances in Physical Chemistry

International Journal of Analytical Chemistry
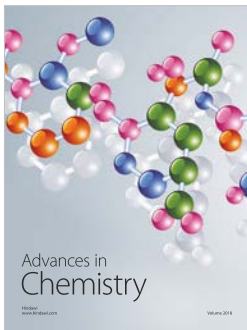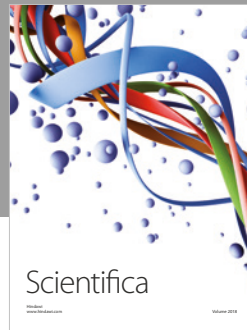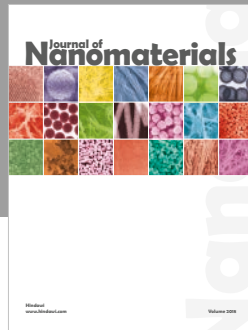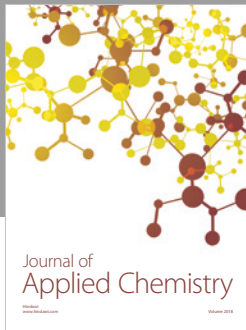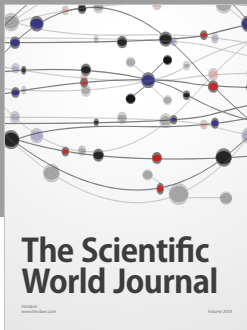
Hindawi

Submit your manuscripts at
www.hindawi.com

Advances in Condensed Matter Physics

Journal of Chemistry

International Journal of Biomaterials

Advances in High Energy Physics

Journal of Engineering

Journal of Nanotechnology

International Journal of Corrosion

Journal of Materials

BioMed Research International

Advances in Tribology

Advances in Materials Science and Engineering